Vector Boson Scattering at CLIC: Determination of anomalous gauge couplings

Christian Fleper

University of Siegen

christian.fleper@uni-siegen.de

January 21, 2016

in collaboration with W. Kilian, T. Ohl, J. Reuter, M. Sekulla

Introduction

- Higgs field is responsible for electroweak symmetry breaking $SU(2)_L \times U(1)_Y \rightarrow U(1)_{em}$
- Details of symmetry breaking still unknown
- Vector boson scattering is sensitive to new physics in the Higgs sector
- New physics: additional resonances or **anomalous couplings**

Effective field theory and anomalous couplings

- $\mathcal{L}_{eff} = \mathcal{L}_{SM} + \sum_i \mathcal{L}_i$
- Relevant longitudinal dimension eight operators:

$$\mathcal{L}_{S,0} = F_{S,0}\mathrm{Tr}[(\mathbf{D}_\mu\mathbf{H})^\dagger(\mathbf{D}_\nu\mathbf{H})]\mathrm{Tr}[(\mathbf{D}^\mu\mathbf{H})^\dagger(\mathbf{D}^\nu\mathbf{H})]$$
$$\mathcal{L}_{S,1} = F_{S,1}\mathrm{Tr}[(\mathbf{D}_\mu\mathbf{H})^\dagger(\mathbf{D}^\mu\mathbf{H})]\mathrm{Tr}[(\mathbf{D}_\nu\mathbf{H})^\dagger(\mathbf{D}^\nu\mathbf{H})]$$

  H linear representation of the Higgs field
- Goal: measure couplings $F_{S,0}$ and $F_{S,1}$

$$\boxed{\mathbf{H} \equiv \frac{1}{2}\begin{pmatrix} v + h - iw^3 & -i\sqrt{2}w^+ \\ -i\sqrt{2}w^- & v + h + iw^3 \end{pmatrix}}$$

Vector boson scattering

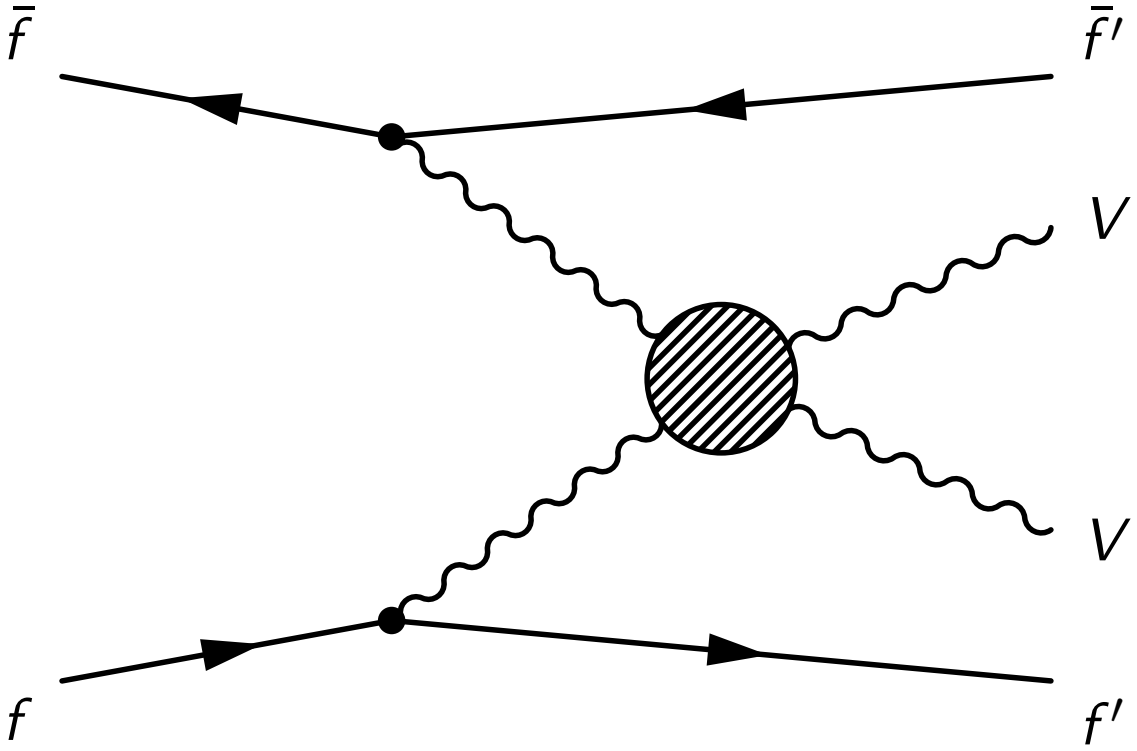

Figure: Feynman diagram for vector boson scattering in a fermion antifermion collision.

Signal and background processes in VBS

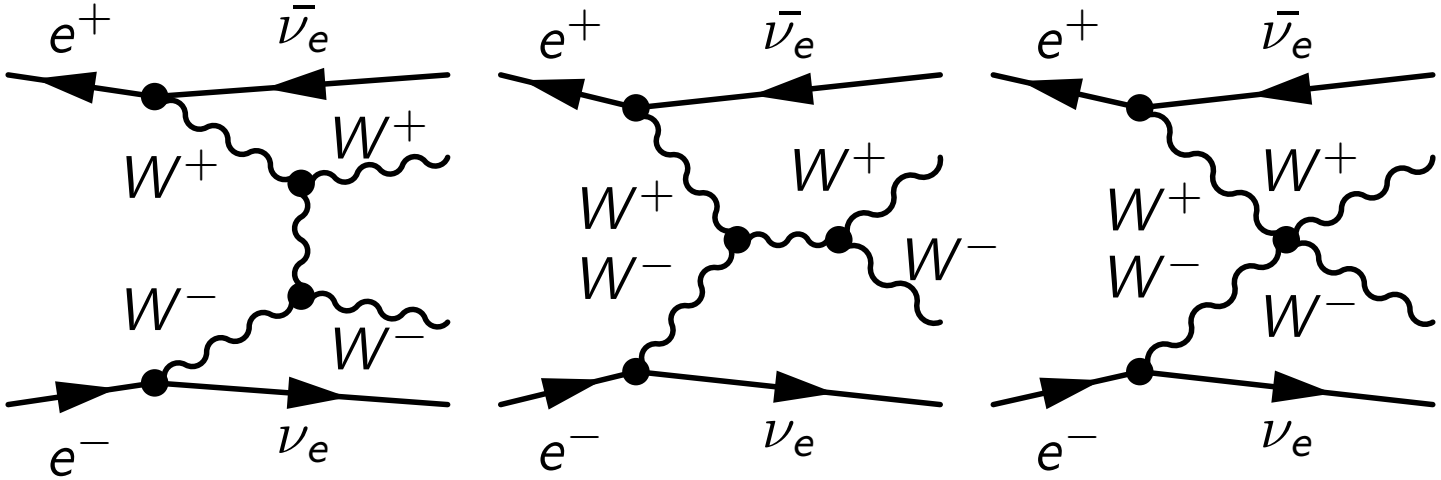

Figure: Feynman diagrams contributing to the vector boson scattering signal.

Signal and background processes in VBS

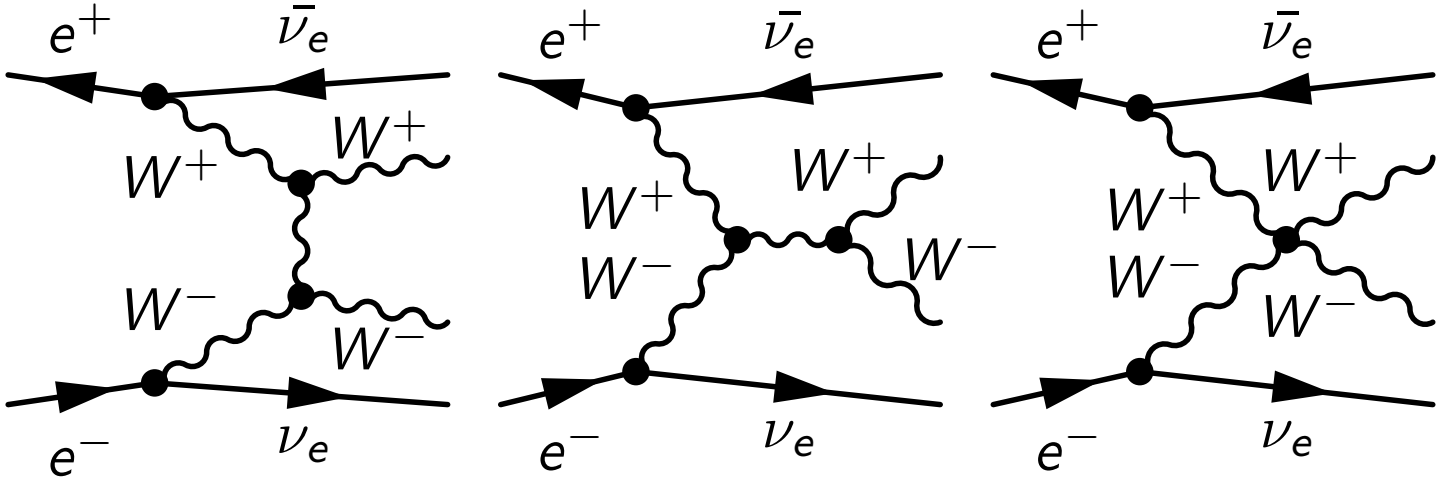

Figure: Feynman diagrams contributing to the vector boson scattering signal.

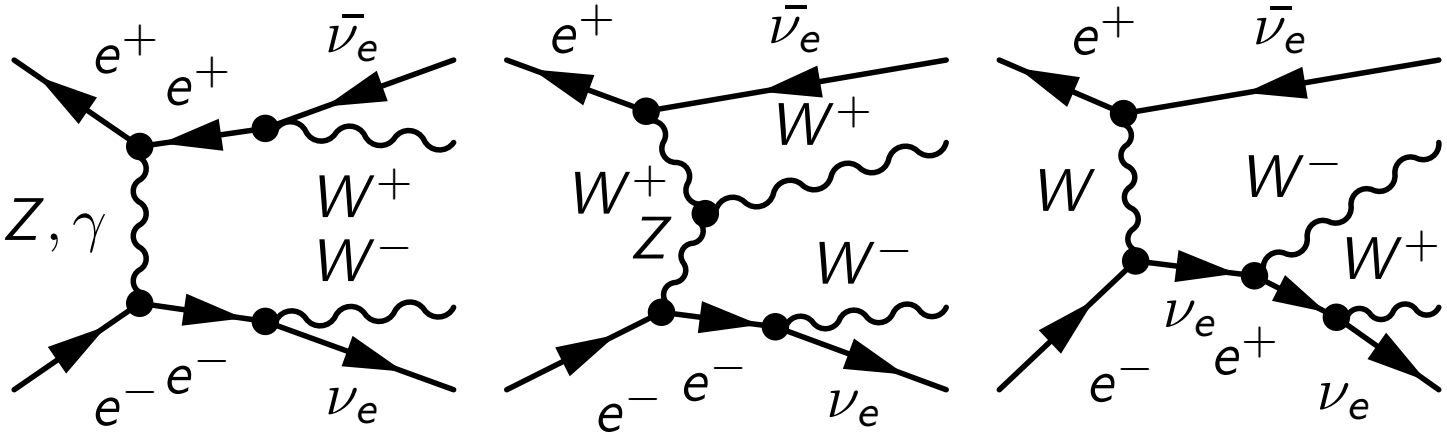

Figure: Feynman diagrams contributing to the irreducible background.

Signal and background processes in VBS

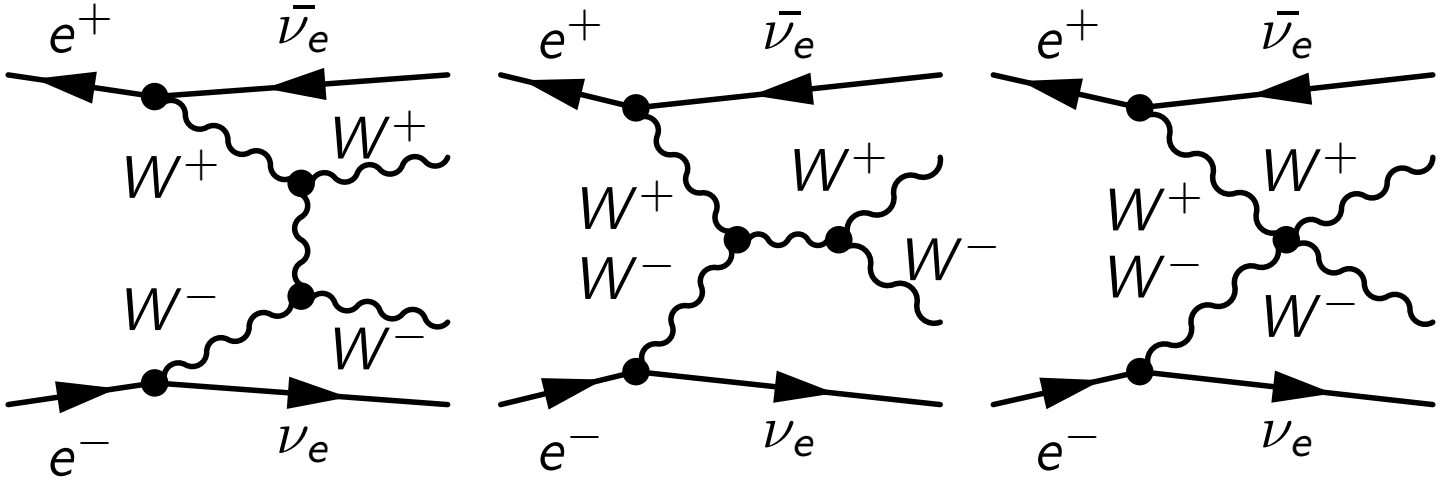

Figure: Feynman diagrams contributing to the vector boson scattering signal.

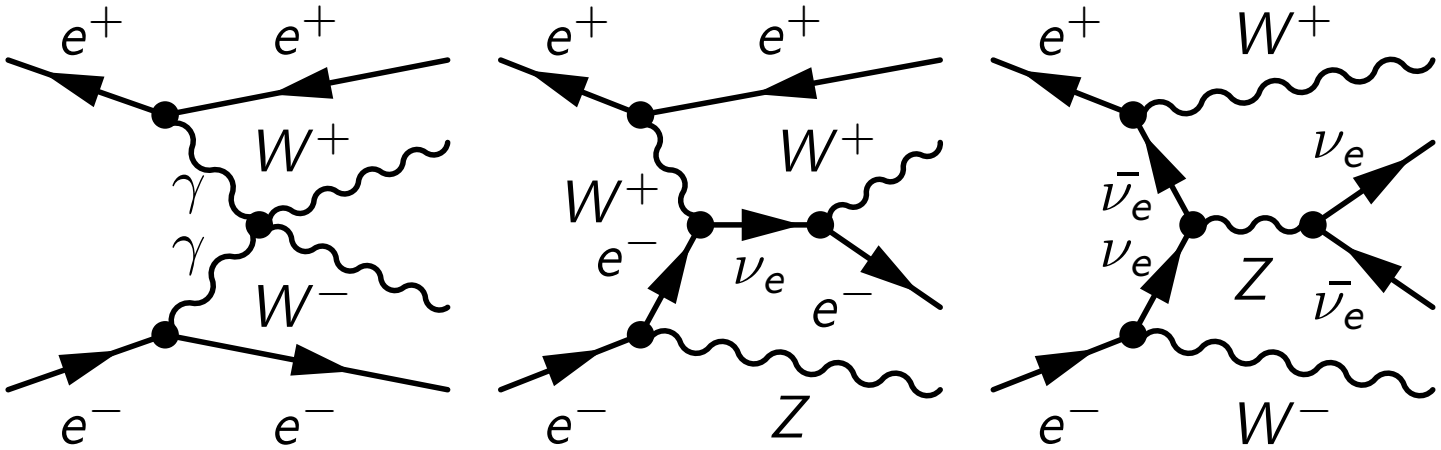

Figure: Feynman diagrams contributing to the partially reducible background.

CLIC

CLIC energy stages and int. luminosities

- $(E_1 = 350/375\,\text{GeV},\ \mathcal{L}_{int,1} = 500\,\text{fb}^{-1})$
- $E_2 = 1400\,\text{GeV},\ \mathcal{L}_{int,2} = 1500\,\text{fb}^{-1}$
- $E_3 = 3000\,\text{GeV},\ \mathcal{L}_{int,3} = 2000\,\text{fb}^{-1}$

CLIC

CLIC energy stages and int. luminosities

- $(E_1 = 350/375\,\text{GeV},\ \mathcal{L}_{int,1} = 500\,\text{fb}^{-1})$
- $E_2 = 1400\,\text{GeV},\ \mathcal{L}_{int,2} = 1500\,\text{fb}^{-1}$
- $E_3 = 3000\,\text{GeV},\ \mathcal{L}_{int,3} = 2000\,\text{fb}^{-1}$

Initial state polarization

e^- : 80%
e^+ : 0%

CLIC

CLIC energy stages and int. luminosities

- $(E_1 = 350/375\,\text{GeV},\ \mathcal{L}_{int,1} = 500\,\text{fb}^{-1})$
- $E_2 = 1400\,\text{GeV},\ \mathcal{L}_{int,2} = 1500\,\text{fb}^{-1}$
- $E_3 = 3000\,\text{GeV},\ \mathcal{L}_{int,3} = 2000\,\text{fb}^{-1}$

Initial state polarization

e^- : 80%
e^+ : 0%

Low angle coverage M. Idzik: DOI: 10.5506/APhysPolB.46.1297

- LumiCal: 38-110 mrad
- BeamCal: 15-38 mrad

CLIC

CLIC energy stages and int. luminosities

- $(E_1 = 350/375\,\text{GeV},\ \mathcal{L}_{int,1} = 500\,\text{fb}^{-1})$
- $E_2 = 1400\,\text{GeV},\ \mathcal{L}_{int,2} = 1500\,\text{fb}^{-1}$
- $E_3 = 3000\,\text{GeV},\ \mathcal{L}_{int,3} = 2000\,\text{fb}^{-1}$

Initial state polarization

e^- : 80%
e^+ : 0%

Low angle coverage M. Idzik: DOI: 10.5506/APhysPolB.46.1297

- LumiCal: 38-110 mrad
- BeamCal: 15-38 mrad

W and Z identification J. S. Marshall, A. Mnnich, M. A. Thomson: arXiv:1209.4039

- $\approx$ 88 % (with photon induced bkg.: 71-79 %)

WHIZARD W. Kilian, T. Ohl, J. Reuter: arXiv: 0708.4233; M. Moretti, T. Ohl, J. Reuter: arXiv: hep-ph/0102195

- Event generator for collider physics
- Matrix element generator O'Mega
- Efficient phase space and event generation
- Current release: 2.2.8 (November 22nd, 2015)

Total cross sections without cuts

Process	1400 GeV	3000 GeV	Factor
$W^+W^-\nu\bar{\nu}$	47.1	132	1
$W^+W^-e^+e^-$	1570	3820	1
$W^\pm Ze^\mp\nu$	138	408	0.136
ZZe^+e^-	3.78	4.70	0.019
$W^+W^-(Z \to \nu\bar{\nu})$	11.7	9.35	1
$ZZ\nu\bar{\nu}$	15.7	57.5	1
ZZe^+e^-	3.78	4.70	1
$W^\pm Ze^\mp\nu$	138	408	0.136
$W^+W^-e^+e^-$	1570	3820	0.019
$ZZ(Z \to \nu\bar{\nu})$	0.484	0.237	1

Table: Total cross sections in fb without cuts (error $\approx 1\%$).

Differential cross sections

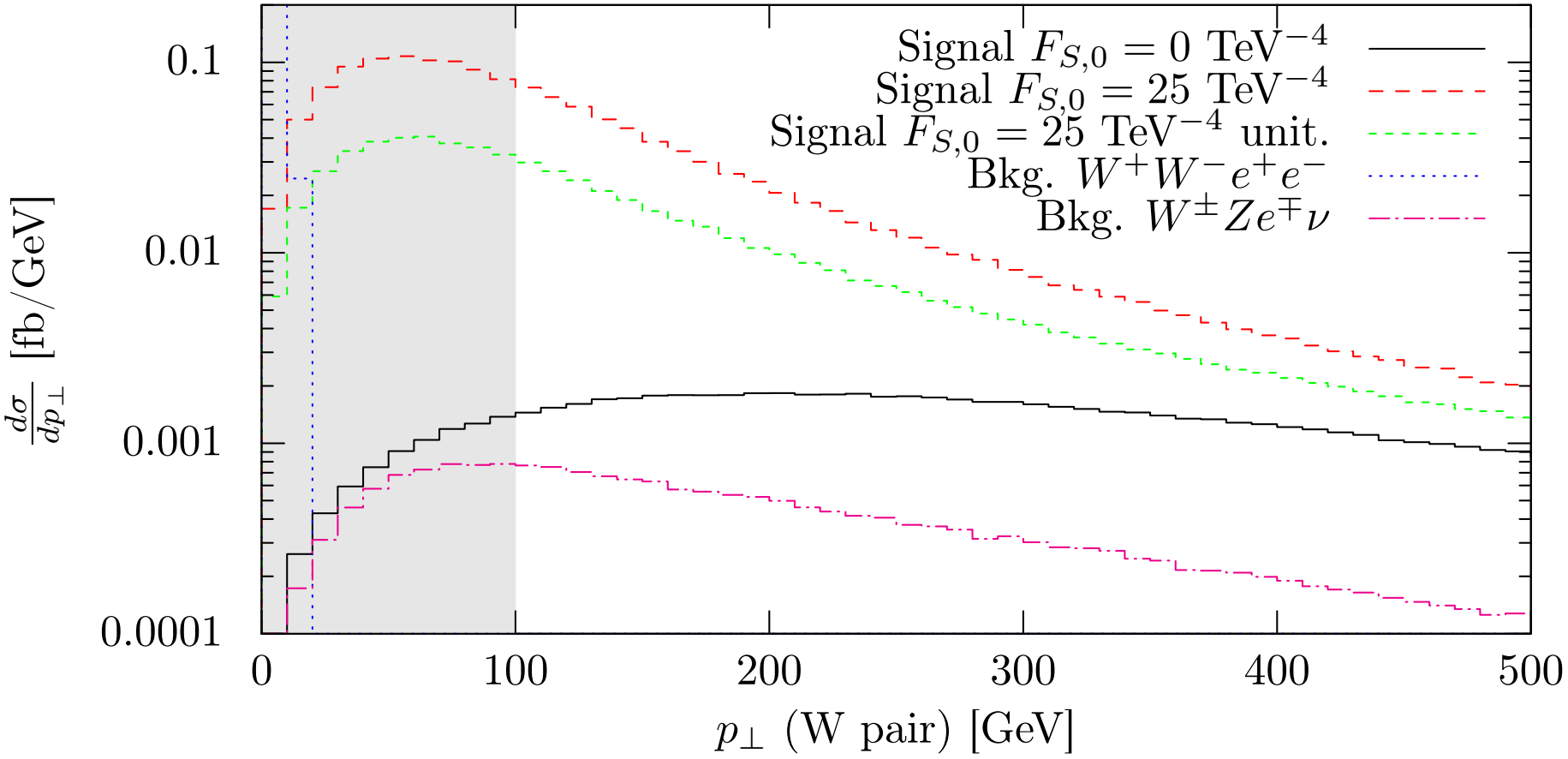

Figure: Differential cross sections depending on the transverse momentum of the W boson pair at $\sqrt{s} = 3000$ GeV.

Used cuts

1. $M_{inv}(\bar{\nu}\nu) > 230(175)\,\text{GeV}$ (neutrinos originate from Z decay, backgrounds from W^+W^- and QCD four-jet production)
2. $|\cos\theta(W/Z)| < 0.8$ and $p_\perp(W/Z) > 300(180)\,\text{GeV}$ (backgrounds which result from t-channel exchange in the subprocess)
3. $\theta(e) > 15\,\text{mrad}$ and $p_\perp(WW) > 100(50)\,\text{GeV}$, $p_\perp(ZZ) > 60(40)\,\text{GeV}$ (background resulting from $\gamma\gamma$ fusion)
4. $900(800)\,\text{GeV} < M_{inv}(WW) < 1900(1175)\,\text{GeV}$, $850(800)\,\text{GeV} < M_{inv}(ZZ) < 1900(1175)\,\text{GeV}$ (non scattered vector bosons)

Cross sections with cuts

Process	1400 GeV	3000 GeV	Factor
$W^+W^-\nu\bar{\nu}$	0.119	0.790	1
$W^+W^-e^+e^-$	0.000	0.000	1
$W^\pm Ze^\mp\nu$	0.269	1.200	0.136
ZZe^+e^-	0.000	0.000	0.019
$W^+W^-(Z \to \nu\bar{\nu})$	0.039	0.610	1
$ZZ\nu\bar{\nu}$	0.084	0.790	1
ZZe^+e^-	0.000	0.000	1
$W^\pm Ze^\mp\nu$	0.288	1.593	0.136
$W^+W^-e^+e^-$	0.000	0.000	0.019
$ZZ(Z \to \nu\bar{\nu})$	0.000	0.000	1

Table: Total cross sections in fb with cuts (error $\approx 1\%$).

Cross sections at 1400 GeV

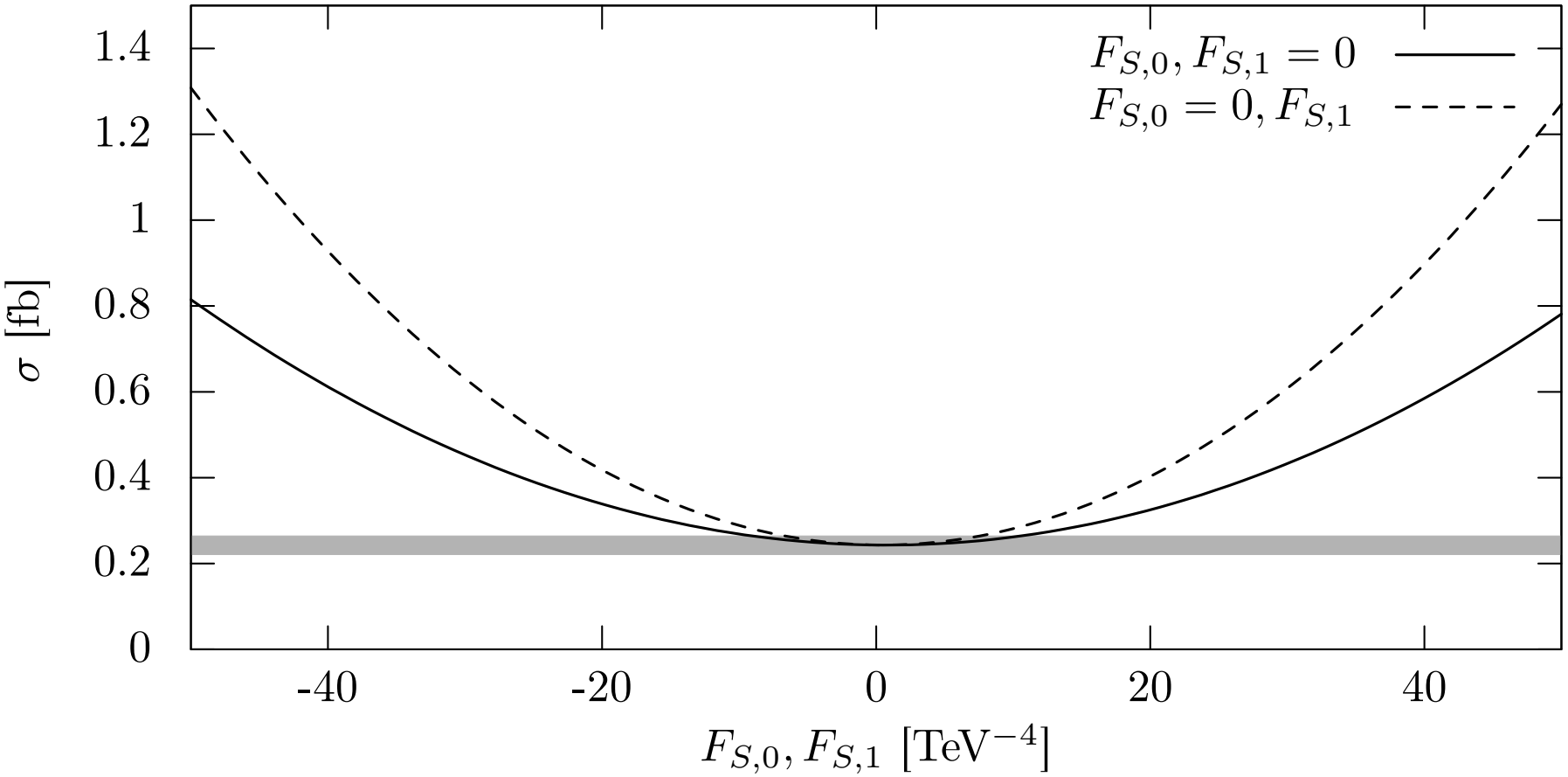

Figure: Total cross sections of $e^+e^- \to W^+W^-\nu\bar{\nu}$ depending on $F_{S,0}$ and $F_{S,1}$ at $\sqrt{s} = 1400\,\text{GeV}$ without unitarization.

Exclusion contours and exclusion sensitivities at 1400 GeV

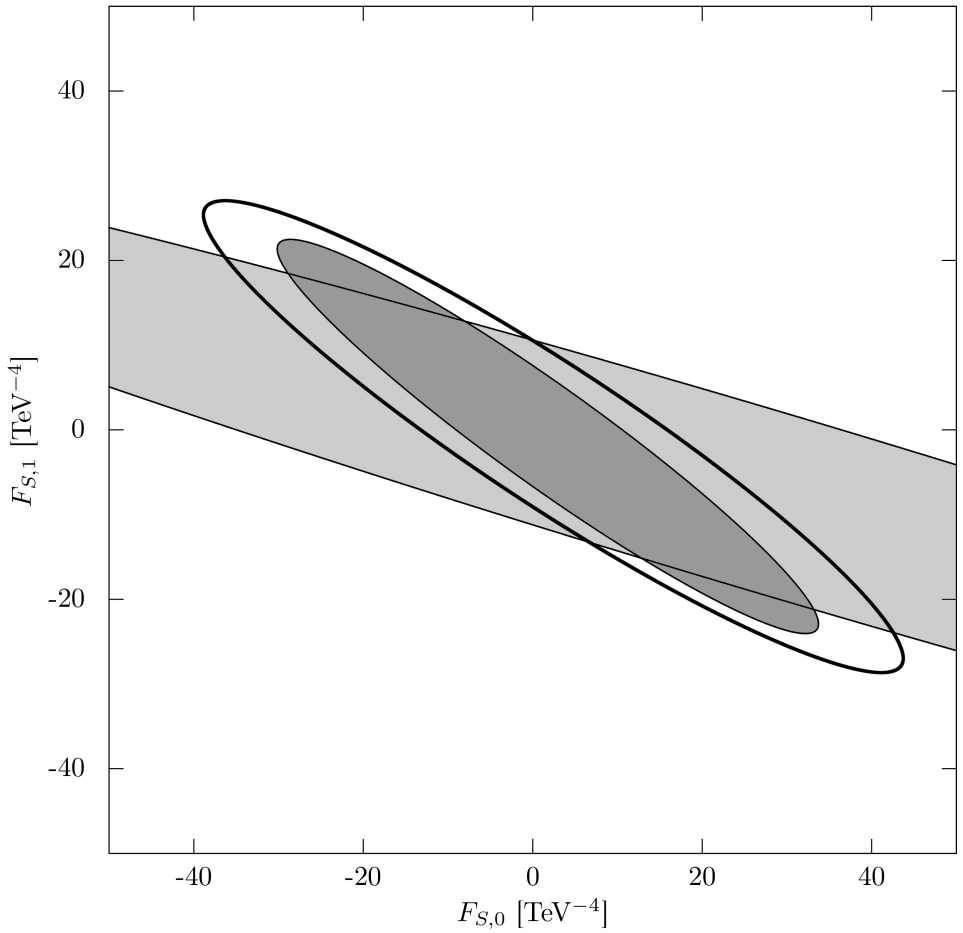

Figure: $\pm 1\sigma$ exclusion contours and 90% exclusion sensitivity in the $F_{S,0}/F_{S,1}$ plane at $\sqrt{s} = 1400\,\text{GeV}$ without unitarization.

Exclusion contours and exclusion sensitivities at 1400 GeV

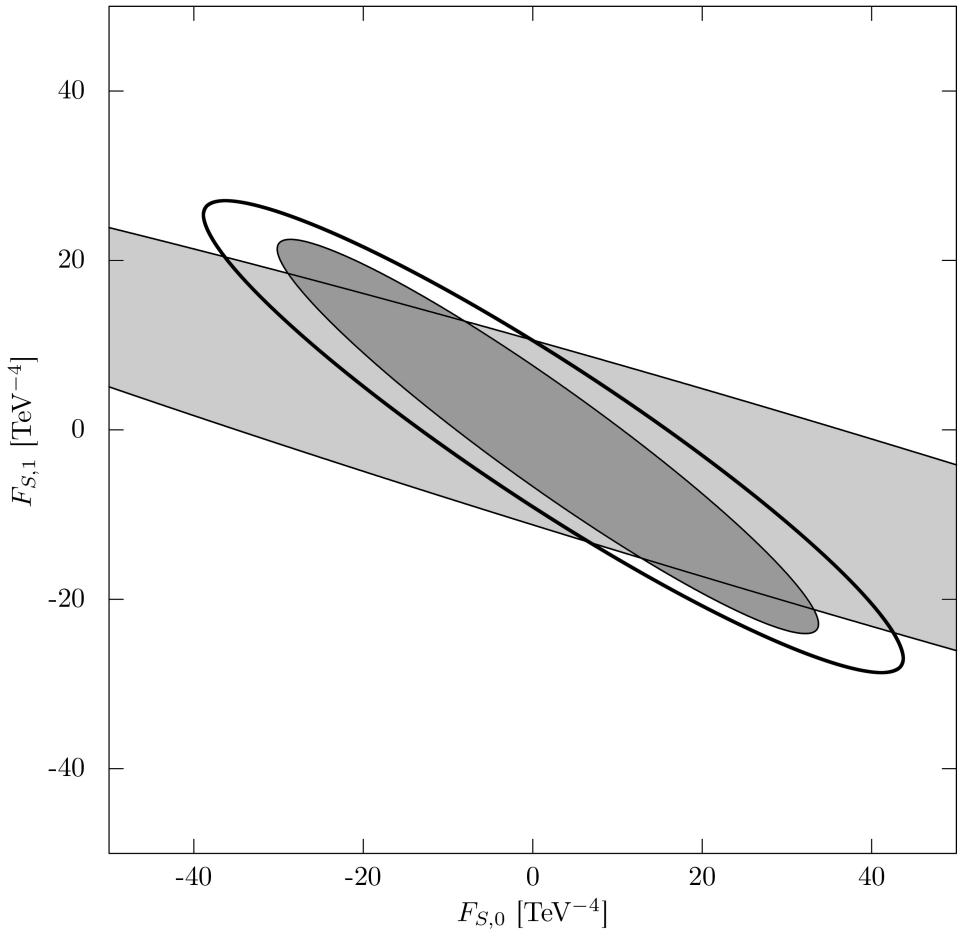

Figure: $\pm 1\sigma$ exclusion contours and 90% exclusion sensitivity in the $F_{S,0}/F_{S,1}$ plane at $\sqrt{s} = 1400\,\text{GeV}$ without unitarization.

$\Rightarrow$ 90% exclusion sensitivity $\approx 30 - 40\,\text{TeV}^{-4}$

Exclusion contours and exclusion sensitivities at 3000 GeV

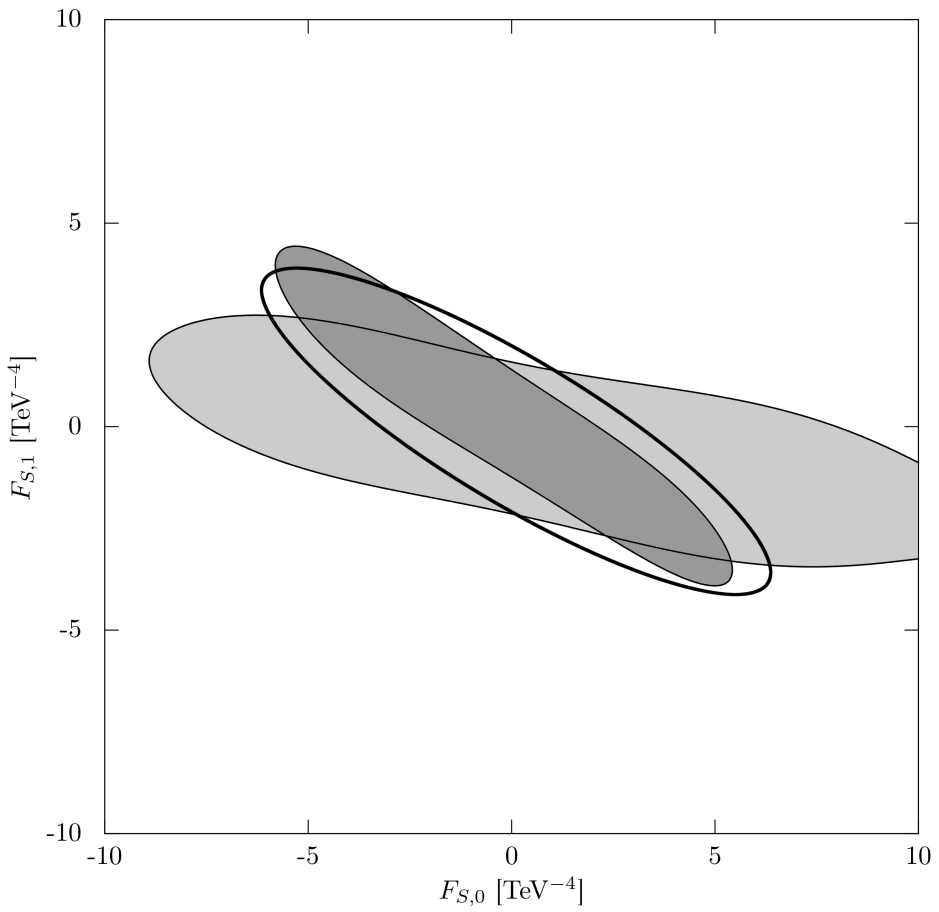

Figure: $\pm 1\sigma$ exclusion contours and 90% exclusion sensitivity in the $F_{S,0}/F_{S,1}$ plane at $\sqrt{s} = 3000\,\text{GeV}$ with unitarization.

Exclusion contours and exclusion sensitivities at 3000 GeV

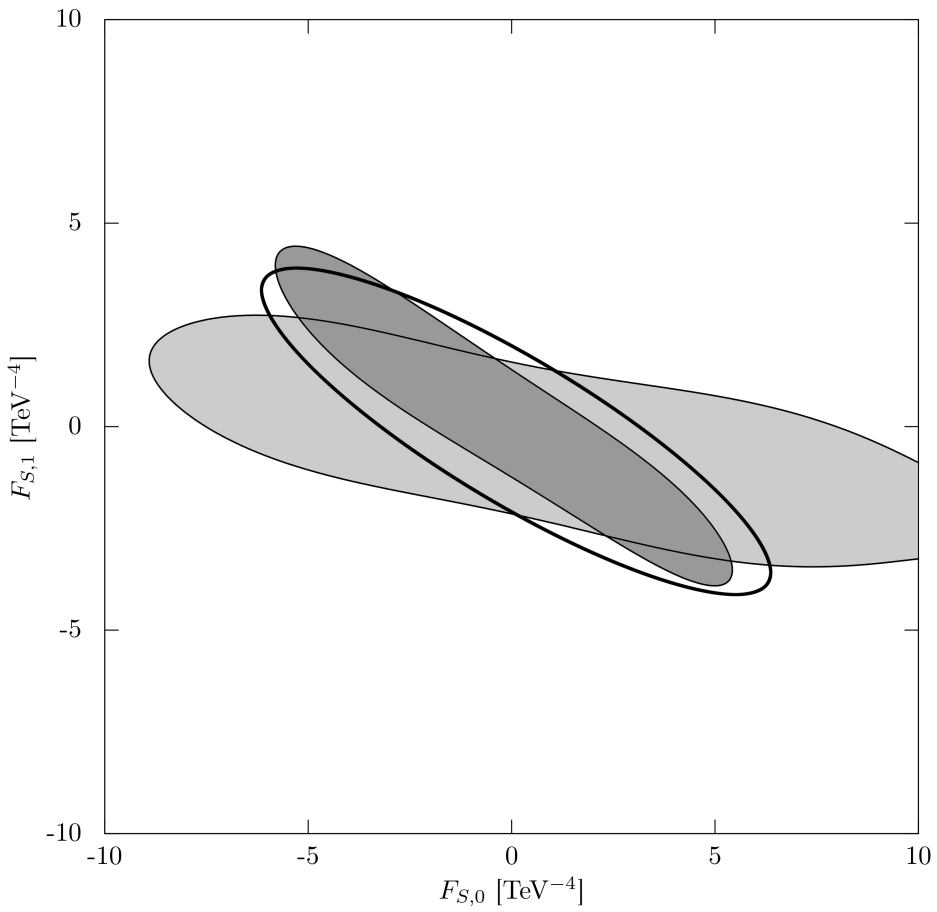

Figure: $\pm 1\sigma$ exclusion contours and 90% exclusion sensitivity in the $F_{S,0}/F_{S,1}$ plane at $\sqrt{s} = 3000\,\text{GeV}$ with unitarization.

$\Rightarrow$ 90% exclusion sensitivity $\approx 5 - 7\,\text{TeV}^{-4}$

Actual values

Theoretical CLIC values

$-40\,\mathrm{TeV}^{-4} < F_{S,0,1} < 40\,\mathrm{TeV}^{-4}$ (1400 GeV)
$-7\,\mathrm{TeV}^{-4} < F_{S,0,1} < 7\,\mathrm{TeV}^{-4}$ (3000 GeV)

Latest ATLAS analysis G. Aad et al.: arXiv:1405.6241

$-461\,\mathrm{TeV}^{-4} < F_{S,0} < 527\,\mathrm{TeV}^{-4}$
$-758\,\mathrm{TeV}^{-4} < F_{S,1} < 791\,\mathrm{TeV}^{-4}$

Actual values

Theoretical CLIC values

$-40\,\mathrm{TeV}^{-4} < F_{S,0,1} < 40\,\mathrm{TeV}^{-4}$ (1400 GeV)
$-7\,\mathrm{TeV}^{-4} < F_{S,0,1} < 7\,\mathrm{TeV}^{-4}$ (3000 GeV)

Latest ATLAS analysis G. Aad et al.: arXiv:1405.6241

$-461\,\mathrm{TeV}^{-4} < F_{S,0} < 527\,\mathrm{TeV}^{-4}$
$-758\,\mathrm{TeV}^{-4} < F_{S,1} < 791\,\mathrm{TeV}^{-4}$

$\Rightarrow$ CLIC values up to 15x (90x) better

Actual values

Theoretical CLIC values

$-40\,\mathrm{TeV}^{-4} < F_{S,0,1} < 40\,\mathrm{TeV}^{-4}$ (1400 GeV)
$-7\,\mathrm{TeV}^{-4} < F_{S,0,1} < 7\,\mathrm{TeV}^{-4}$ (3000 GeV)

Latest ATLAS analysis G. Aad et al.: arXiv:1405.6241

$-461\,\mathrm{TeV}^{-4} < F_{S,0} < 527\,\mathrm{TeV}^{-4}$
$-758\,\mathrm{TeV}^{-4} < F_{S,1} < 791\,\mathrm{TeV}^{-4}$

$\Rightarrow$ CLIC values up to 15x (90x) better

Max. photon induced bkg.: exclusion sensitivities worsen $\approx 15 - 20\%$

Conclusion

- CLIC offers great possibilities for measuring anomalous gauge couplings.
- Exclusion sensitivities can be enhanced.
- Measurements are complementary to the LHC measurements.
- Especially BeamCal and LumiCal detectors important to reduce background.

Outlook

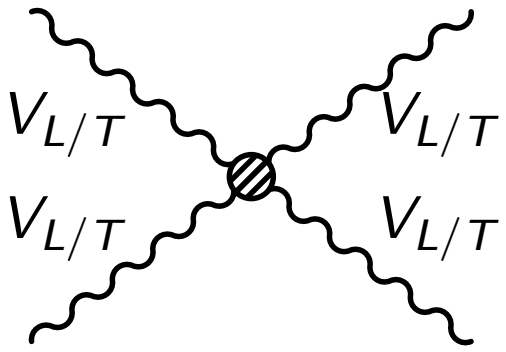

Figure: Scattering of longitudinal/transverse vector bosons.

Relevant Operators:

- $\mathcal{L}_{S,0} = F_{S,0}\mathrm{Tr}[(\mathbf{D}_\mu\mathbf{H})^\dagger(\mathbf{D}_\nu\mathbf{H})]\mathrm{Tr}[(\mathbf{D}^\mu\mathbf{H})^\dagger(\mathbf{D}^\nu\mathbf{H})]$
- $\mathcal{L}_{S,1} = F_{S,1}\mathrm{Tr}[(\mathbf{D}_\mu\mathbf{H})^\dagger(\mathbf{D}^\mu\mathbf{H})]\mathrm{Tr}[(\mathbf{D}_\nu\mathbf{H})^\dagger(\mathbf{D}^\nu\mathbf{H})]$

Outlook

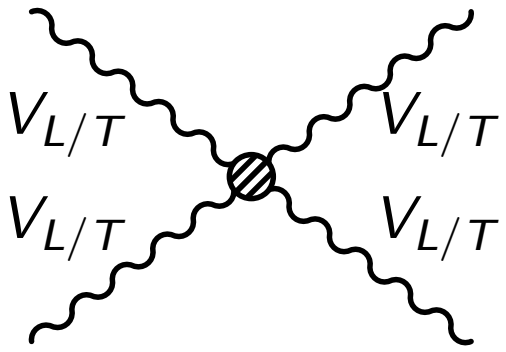

Figure: Scattering of longitudinal/transverse vector bosons.

Relevant Operators:

- $\mathcal{L}_{S,0} = F_{S,0}\mathrm{Tr}[(\mathbf{D}_\mu\mathbf{H})^\dagger(\mathbf{D}_\nu\mathbf{H})]\mathrm{Tr}[(\mathbf{D}^\mu\mathbf{H})^\dagger(\mathbf{D}^\nu\mathbf{H})]$
- $\mathcal{L}_{S,1} = F_{S,1}\mathrm{Tr}[(\mathbf{D}_\mu\mathbf{H})^\dagger(\mathbf{D}^\mu\mathbf{H})]\mathrm{Tr}[(\mathbf{D}_\nu\mathbf{H})^\dagger(\mathbf{D}^\nu\mathbf{H})]$
- $\mathcal{L}_{M,0} = -g^2 F_{M,0}\mathrm{Tr}[(\mathbf{D}_\mu\mathbf{H})^\dagger(\mathbf{D}^\mu\mathbf{H})]\mathrm{Tr}[\mathbf{W}_{\nu\rho}\mathbf{W}^{\nu\rho}]$
- $\mathcal{L}_{M,1} = -g^2 F_{M,1}\mathrm{Tr}[(\mathbf{D}_\mu\mathbf{H})^\dagger(\mathbf{D}^\rho\mathbf{H})]\mathrm{Tr}[\mathbf{W}_{\nu\rho}\mathbf{W}^{\nu\mu}]$

Outlook

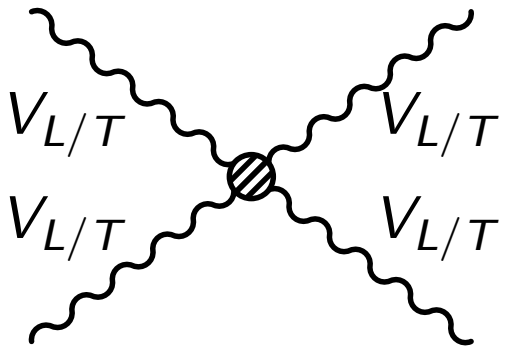

Figure: Scattering of longitudinal/transverse vector bosons.

Relevant Operators:

- $\mathcal{L}_{S,0} = F_{S,0}\mathrm{Tr}[(\mathbf{D}_\mu\mathbf{H})^\dagger(\mathbf{D}_\nu\mathbf{H})]\mathrm{Tr}[(\mathbf{D}^\mu\mathbf{H})^\dagger(\mathbf{D}^\nu\mathbf{H})]$
- $\mathcal{L}_{S,1} = F_{S,1}\mathrm{Tr}[(\mathbf{D}_\mu\mathbf{H})^\dagger(\mathbf{D}^\mu\mathbf{H})]\mathrm{Tr}[(\mathbf{D}_\nu\mathbf{H})^\dagger(\mathbf{D}^\nu\mathbf{H})]$
- $\mathcal{L}_{M,0} = -g^2 F_{M,0}\mathrm{Tr}[(\mathbf{D}_\mu\mathbf{H})^\dagger(\mathbf{D}^\mu\mathbf{H})]\mathrm{Tr}[\mathbf{W}_{\nu\rho}\mathbf{W}^{\nu\rho}]$
- $\mathcal{L}_{M,1} = -g^2 F_{M,1}\mathrm{Tr}[(\mathbf{D}_\mu\mathbf{H})^\dagger(\mathbf{D}^\rho\mathbf{H})]\mathrm{Tr}[\mathbf{W}_{\nu\rho}\mathbf{W}^{\nu\mu}]$
- $\mathcal{L}_{T,0} = g^4 F_{T,0}\mathrm{Tr}[\mathbf{W}_{\mu\nu}\mathbf{W}^{\mu\nu}]\mathrm{Tr}[\mathbf{W}_{\alpha\beta}\mathbf{W}^{\alpha\beta}]$
- $\mathcal{L}_{T,1} = g^4 F_{T,1}\mathrm{Tr}[\mathbf{W}_{\alpha\nu}\mathbf{W}^{\mu\beta}]\mathrm{Tr}[\mathbf{W}_{\mu\beta}\mathbf{W}^{\alpha\nu}]$
- $\mathcal{L}_{T,2} = g^4 F_{T,2}\mathrm{Tr}[\mathbf{W}_{\alpha\mu}\mathbf{W}^{\mu\beta}]\mathrm{Tr}[\mathbf{W}_{\beta\nu}\mathbf{W}^{\nu\alpha}]$

Outlook

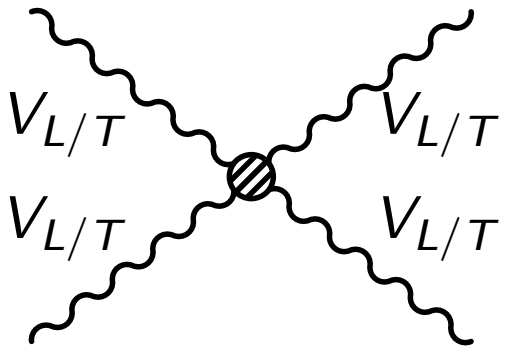

Figure: Scattering of longitudinal/transverse vector bosons.

Relevant Operators:

- $\mathcal{L}_{S,0} = F_{S,0}\mathrm{Tr}[(\mathbf{D}_\mu\mathbf{H})^\dagger(\mathbf{D}_\nu\mathbf{H})]\mathrm{Tr}[(\mathbf{D}^\mu\mathbf{H})^\dagger(\mathbf{D}^\nu\mathbf{H})]$
- $\mathcal{L}_{S,1} = F_{S,1}\mathrm{Tr}[(\mathbf{D}_\mu\mathbf{H})^\dagger(\mathbf{D}^\mu\mathbf{H})]\mathrm{Tr}[(\mathbf{D}_\nu\mathbf{H})^\dagger(\mathbf{D}^\nu\mathbf{H})]$
- $\mathcal{L}_{M,0} = -g^2 F_{M,0}\mathrm{Tr}[(\mathbf{D}_\mu\mathbf{H})^\dagger(\mathbf{D}^\mu\mathbf{H})]\mathrm{Tr}[\mathbf{W}_{\nu\rho}\mathbf{W}^{\nu\rho}]$
- $\mathcal{L}_{M,1} = -g^2 F_{M,1}\mathrm{Tr}[(\mathbf{D}_\mu\mathbf{H})^\dagger(\mathbf{D}^\rho\mathbf{H})]\mathrm{Tr}[\mathbf{W}_{\nu\rho}\mathbf{W}^{\nu\mu}]$
- $\mathcal{L}_{T,0} = g^4 F_{T,0}\mathrm{Tr}[\mathbf{W}_{\mu\nu}\mathbf{W}^{\mu\nu}]\mathrm{Tr}[\mathbf{W}_{\alpha\beta}\mathbf{W}^{\alpha\beta}]$
- $\mathcal{L}_{T,1} = g^4 F_{T,1}\mathrm{Tr}[\mathbf{W}_{\alpha\nu}\mathbf{W}^{\mu\beta}]\mathrm{Tr}[\mathbf{W}_{\mu\beta}\mathbf{W}^{\alpha\nu}]$
- $\mathcal{L}_{T,2} = g^4 F_{T,2}\mathrm{Tr}[\mathbf{W}_{\alpha\mu}\mathbf{W}^{\mu\beta}]\mathrm{Tr}[\mathbf{W}_{\beta\nu}\mathbf{W}^{\nu\alpha}]$

Unitarization done, now: Implementation in `WHIZARD`.

BACKUP SLIDES

Vector boson scattering

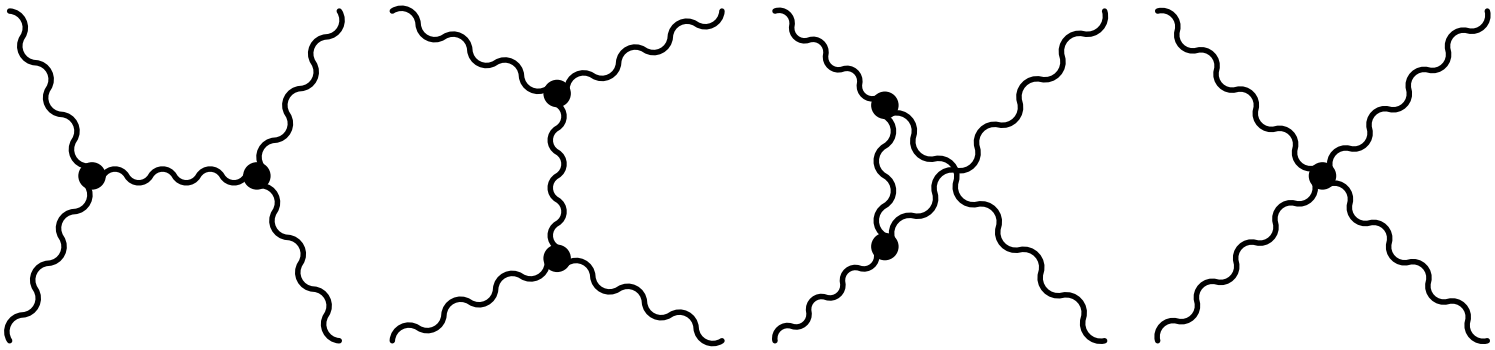

Figure: Feynman diagrams for elastic vector boson scattering with four-point-interaction or a vector boson propagator.

Vector boson scattering

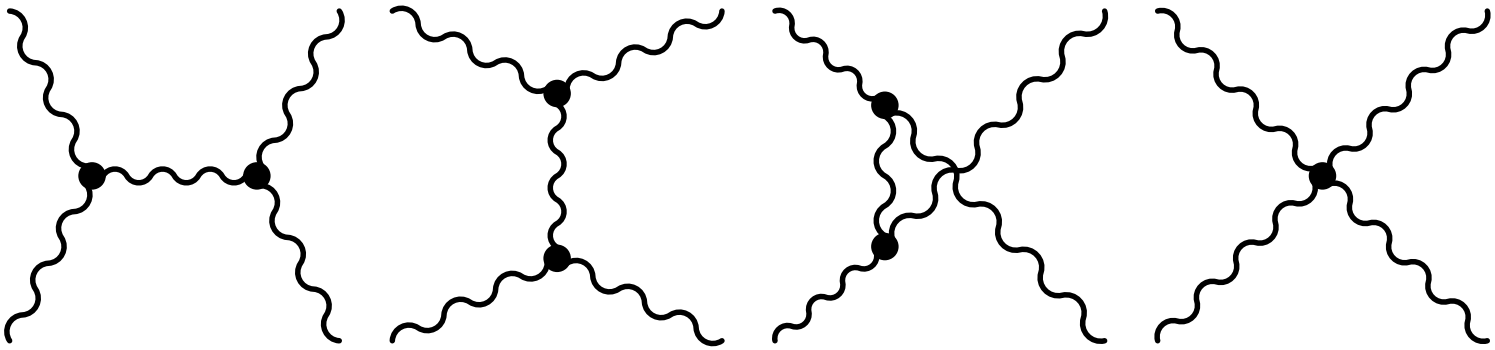

Figure: Feynman diagrams for elastic vector boson scattering with four-point-interaction or a vector boson propagator.

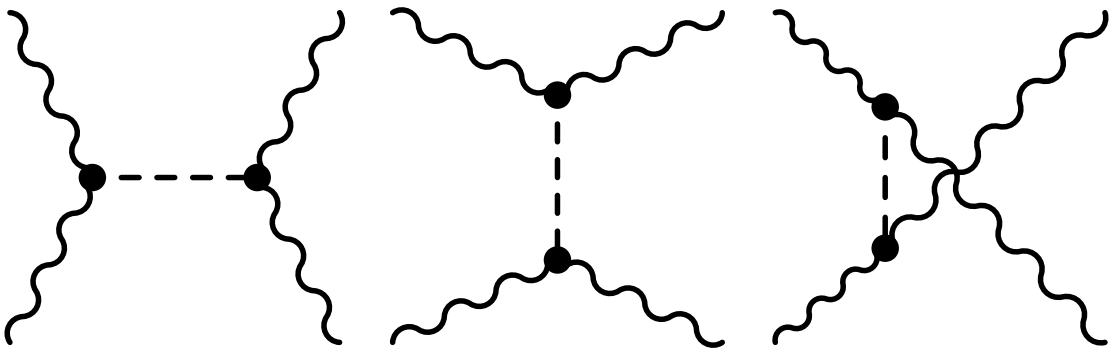

Figure: Feynman diagrams for elastic vector boson scattering with a Higgs propagator.

Differential cross sections

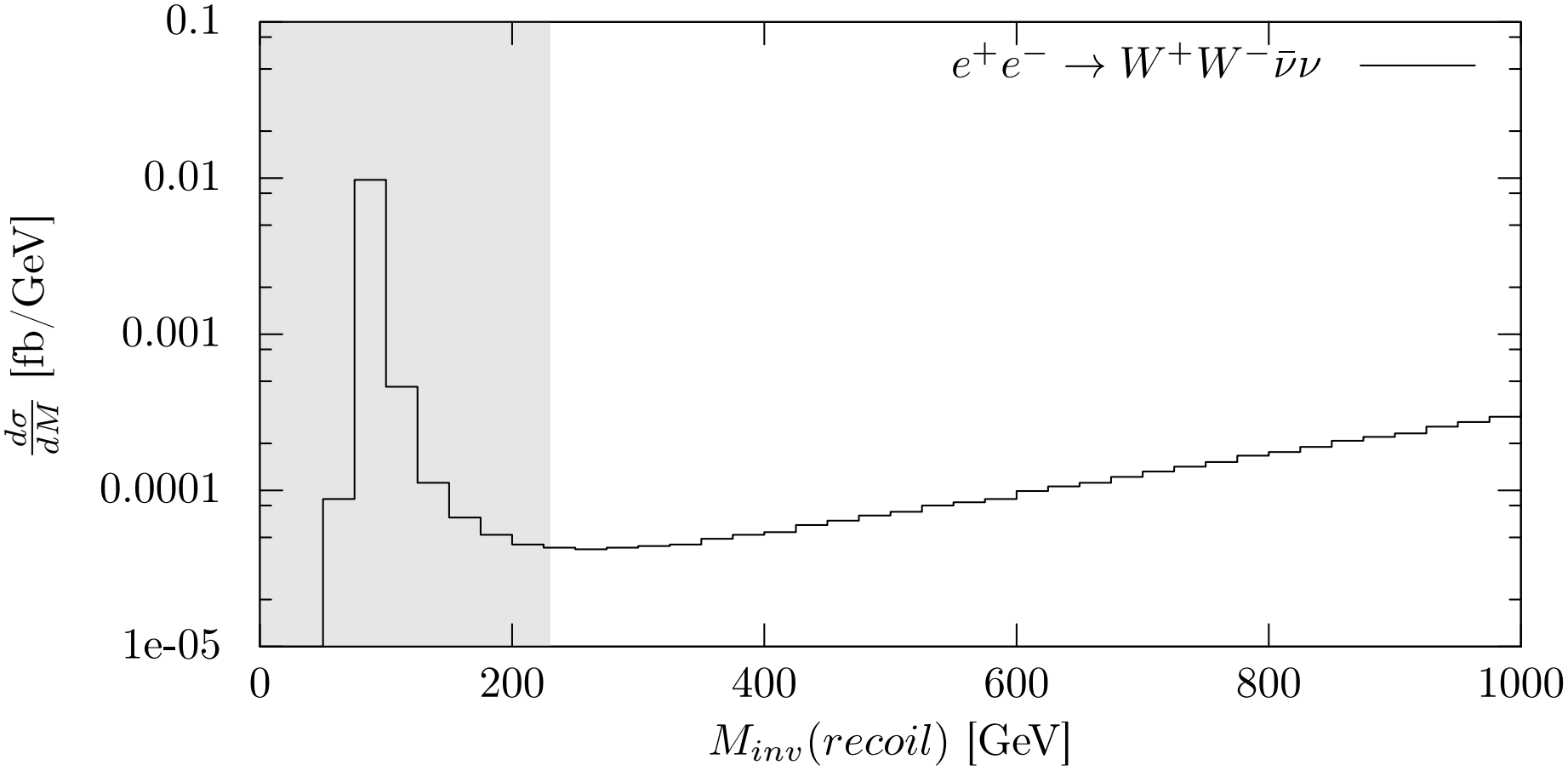

Figure: Differential cross section depending on the W boson pair recoil mass at $\sqrt{s} = 3000\,\text{GeV}$.

Differential cross sections

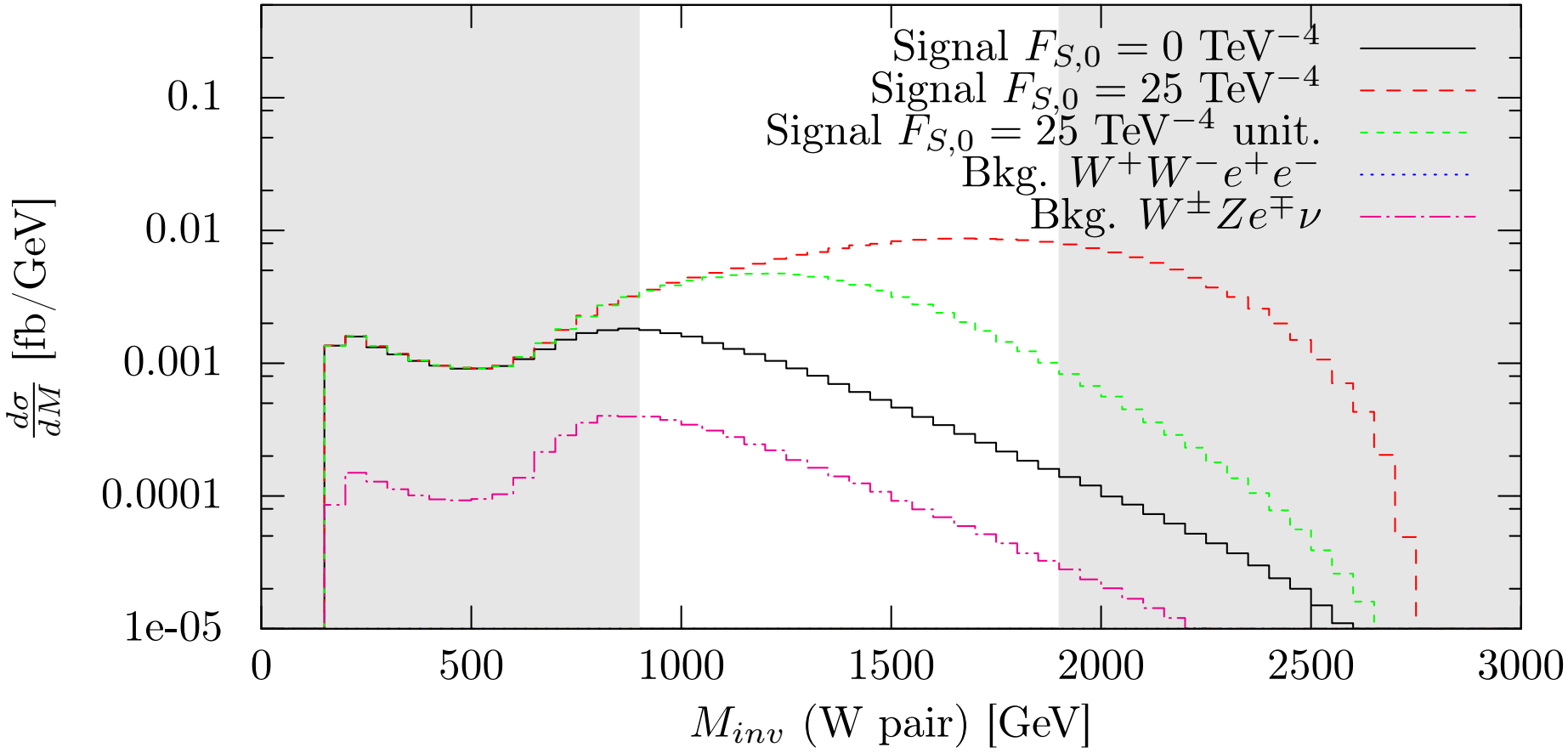

Figure: Differential cross sections depending on the invariant mass of the W boson pair at $\sqrt{s} = 3000$ GeV.

Cross sections at 1400 GeV

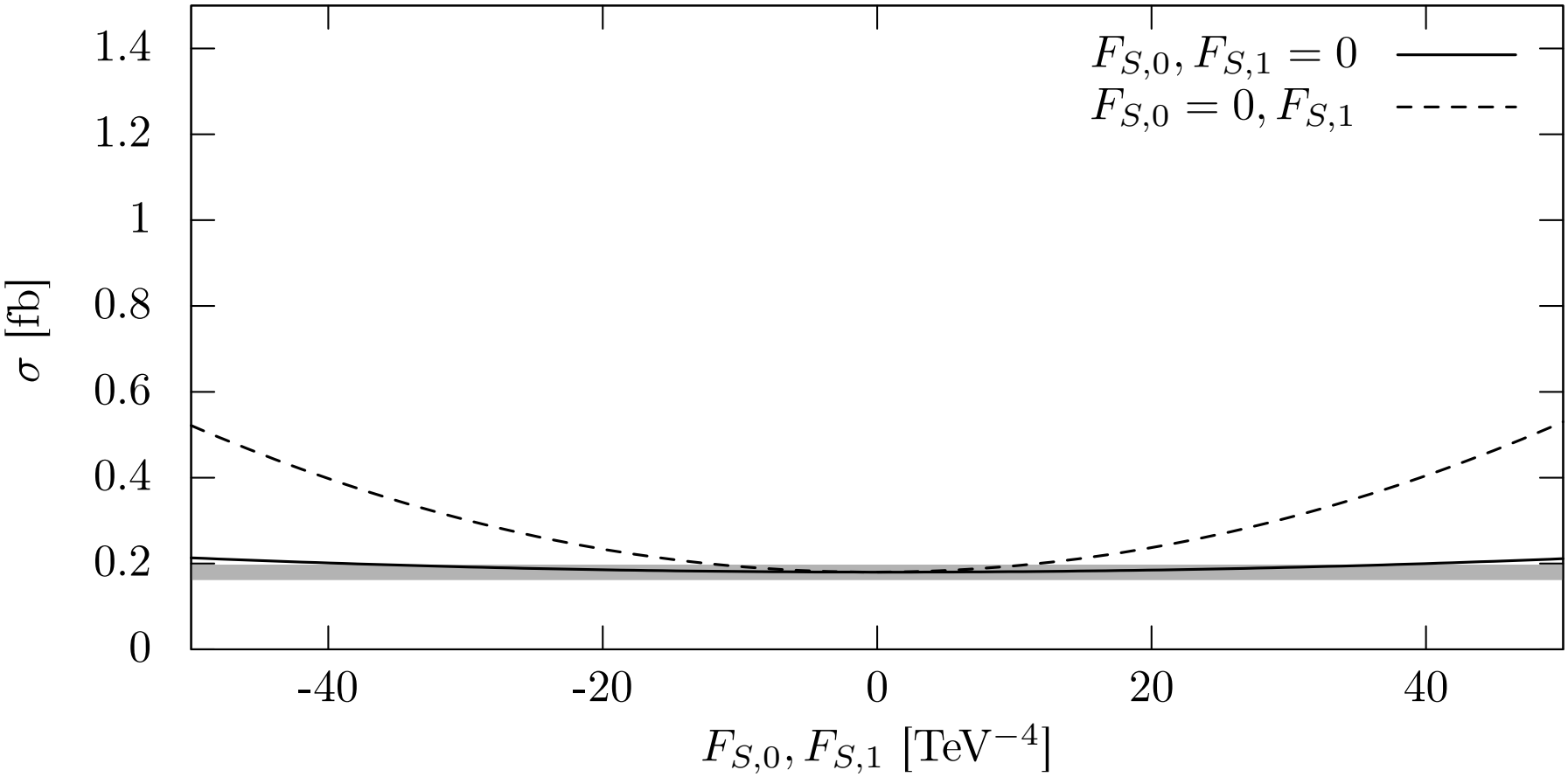

Figure: Total cross sections of $e^+e^- \to ZZ\nu\bar{\nu}$ depending on $F_{S,0}$ and $F_{S,1}$ at $\sqrt{s} = 1400\,\text{GeV}$ without unitarization.

Cross sections at 3000 GeV

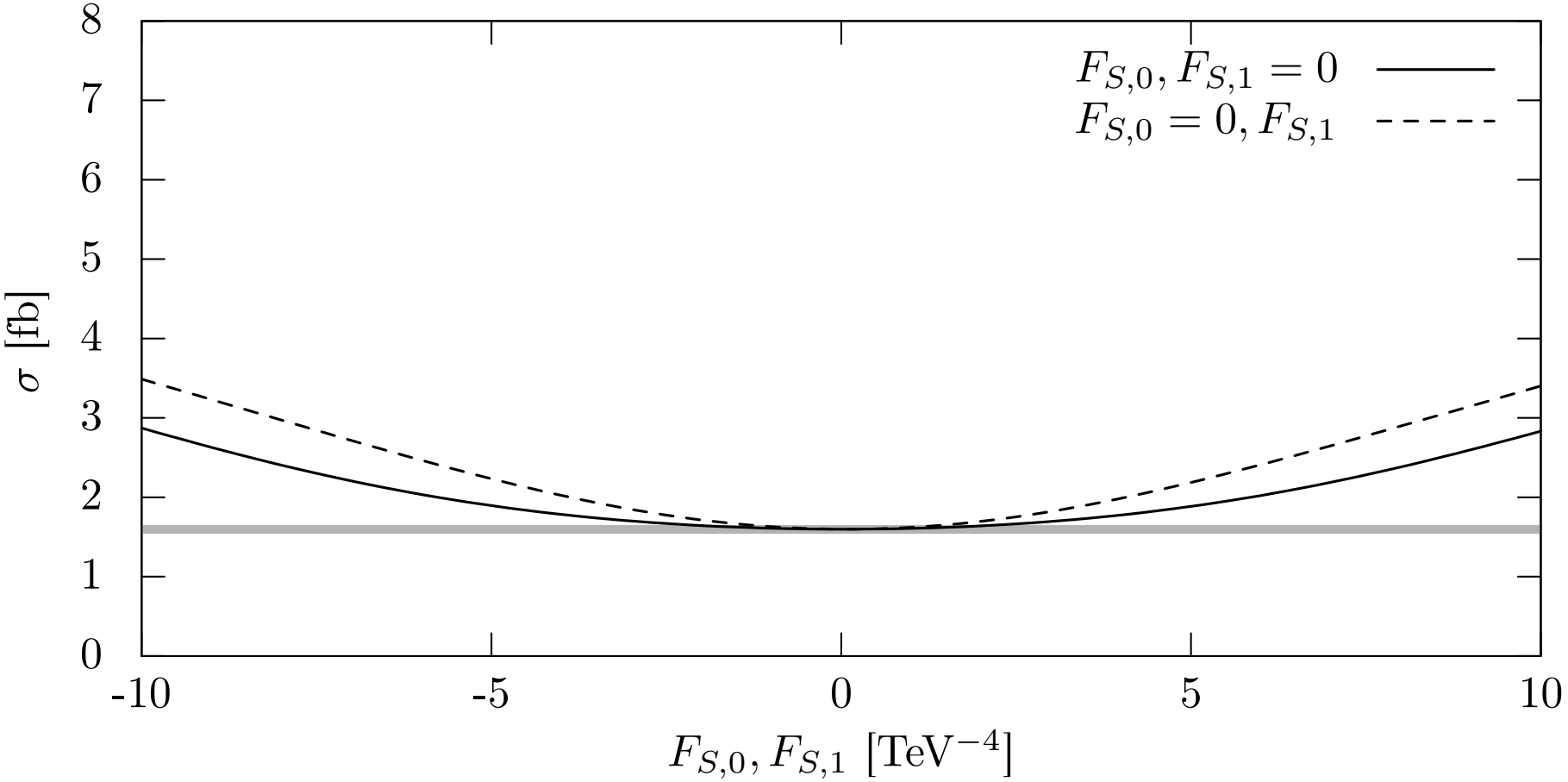

Figure: Total cross sections of $e^+e^- \to W^+W^-\nu\bar{\nu}$ depending on $F_{S,0}$ and $F_{S,1}$ at $\sqrt{s} = 3000\,\text{GeV}$ with unitarization.

Cross sections at 3000 GeV

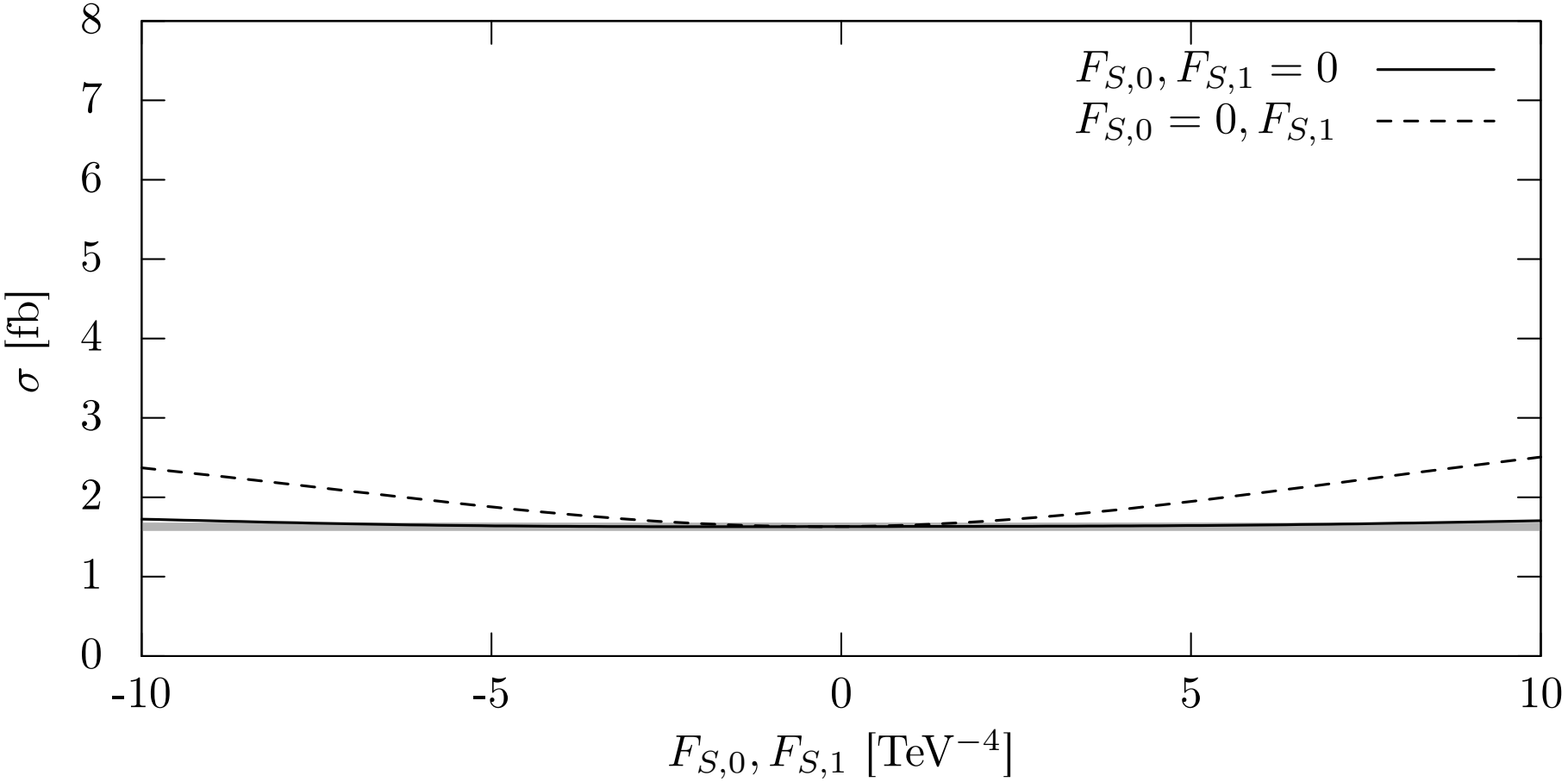

Figure: Total cross sections of $e^+e^- \to ZZ\nu\bar{\nu}$ depending on $F_{S,0}$ and $F_{S,1}$ at $\sqrt{s} = 3000\,\text{GeV}$ with unitarization.